BMES BIOMEDICAL ENGINEERING SOCIETY

ORIGINAL ARTICLE

Preparation of Decellularized Tissue as Dual Cell Carrier Systems: A Step Towards Facilitating Re-epithelization and Cell Encapsulation for Tracheal Reconstruction

Pensuda Sompunga[1] · Watchareewan Rodprasert[2,3] · Sayamon Srisuwatanasagul[4] · Somporn Techangamsuwan[5] · Sirinee Jirajessada[6] · Rattanavinan Hanchaina[7] · Thaned Kangsamaksin[7] · Supansa Yodmuang[8,9,10,11] · Chenphop Sawangmake[2,3,12]

Abstract

Surgical treatment of tracheal diseases, trauma, and congenital stenosis has shown success through tracheal reconstruction coupled with palliative care. However, challenges in surgical-based tracheal repairs have prompted the exploration of alternative approaches for tracheal replacement. Tissue-based treatments, involving the cultivation of patient cells on a network of extracellular matrix (ECM) from donor tissue, hold promise for restoring tracheal structure and function without eliciting an immune reaction. In this study, we utilized decellularized canine tracheas as tissue models to develop two types of cell carriers: a decellularized scaffold and a hydrogel. Our hypothesis posits that both carriers, containing essential biochemical niches provided by ECM components, facilitate cell attachment without inducing cytotoxicity. Canine tracheas underwent vacuum-assisted decellularization (VAD), and the ECM-rich hydrogel was prepared through peptic digestion of the decellularized trachea. The decellularized canine trachea exhibited a significant reduction in DNA content and major histocompatibility complex class II, while preserving crucial ECM components such as collagen, glycosaminoglycan, laminin, and fibronectin. Scanning electron microscope and fluorescent microscope images revealed a fibrous ECM network on the luminal side of the cell-free trachea, supporting epithelial cell attachment. Moreover, the ECM-rich hydrogel exhibited excellent viability for human mesenchymal stem cells encapsulated for 3 days, indicating the potential of cell-laden hydrogel in promoting the

---

Associate Editor Stefan M. Duma oversaw the review of this article.

✉ Supansa Yodmuang
supansa.y@chula.ac.th

✉ Chenphop Sawangmake
chenphop@gmail.com

1 Medical Sciences Program, Faculty of Medicine, Chulalongkorn University, Pathumwan, Bangkok 10330, Thailand

2 Veterinary Stem Cell and Bioengineering Innovation Center (VSCBIC), Faculty of Veterinary Science, Chulalongkorn University, Bangkok 10330, Thailand

3 Veterinary Stem Cell and Bioengineering Research Unit, Faculty of Veterinary Science, Chulalongkorn University, Bangkok 10330, Thailand

4 Department of Anatomy, Faculty of Veterinary Science, Chulalongkorn University, Pathumwan, Bangkok 10330, Thailand

5 Department of Pathology, Faculty of Veterinary Science, Chulalongkorn University, Pathumwan, Bangkok 10330, Thailand

6 Biology Program, Faculty of Science, Buriram Rajabhat University, Muang, Buriram 31000, Thailand

7 Department of Biochemistry, Faculty of Science, Mahidol University, Bangkok 10400, Thailand

8 Research Affairs, Faculty of Medicine, Chulalongkorn University, Ananda Mahidol Building, 1873 Rama 4 Rd, Pathumwan, Bangkok 10330, Thailand

9 Center of Excellence in Biomaterial Engineering for Medical and Health, Chulalongkorn University, Pathumwan, Bangkok 10330, Thailand

10 Clinical Excellence Center for Advanced Therapy Medicinal Products, King Chulalongkorn Memorial Hospital, Pathumwan, Bangkok 10330, Thailand

11 Avatar Biotech for Oral Health & Healthy Longevity Research Unit, Chulalongkorn University, Pathumwan, Bangkok 10330, Thailand

12 Department of Pharmacology, Faculty of Veterinary Science, Chulalongkorn University, Bangkok 10330, Thailand

∅ Springer

development of cartilage rings of the trachea. This study underscores the versatility of the trachea in producing two distinct cell carriers—decellularized scaffold and hydrogel—both containing the native biochemical niche essential for tracheal tissue engineering applications.

Graphical Abstract

Canine tracheae were harvested and subjected to decellularization. The resulting decellularized tracheae were used to prepare two different cell-carrier systems: scaffold and hydrogel. The scaffold was utilized for seeding human bronchial airway epithelium cells (HBEpCs) on the luminal surface, while the hydrogel was used for encapsulating hMSCs and seeding human umbilical vein endothelial cells (HUVECs). The extracellular matrix-rich cell scaffolds provided a biological niche for re-epithelial lining. hMSCs and HUVECs showed remarkable viability in and on the hydrogel, respectively. However, the formation of capillary-like structures by HUVECs was not detected.
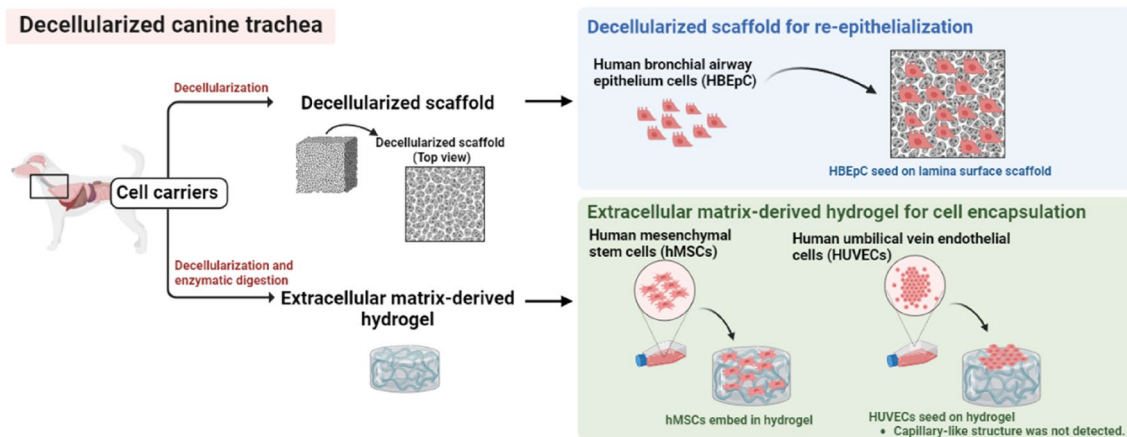
Introduction

Tracheal reconstruction is a complex surgical technique aiming to restore the airway in patients with tracheal injuries or defects. The challenges lie in replicating the tubular shape, structural rigidity, and maintaining a blood supply [1–3]. The limitations of end-to-end anastomosis, the most common technique for sewing the two ends of the trachea together, involve the requirement that the length of trachea resected be shorter than 50% in adults or 30% in children [3–7], the need for a large area of healthy tissue, the possibility of an air leak, and the risk of postoperative stenosis due to tissue tension and scar formation [8–11]. The complexity of surgical-based tracheal repairs has led to the exploration of alternative methods for tracheal replacement.

Tissue engineering has enabled the development of tissue and organ substitutes with the capability to restore and maintain normal function. Engineering tissue architecture for tracheal substitutes is complicated, as it must replicate the intricate structure, biochemical components, and biomechanical properties of the native trachea. Many attempts have been made to address these problems by constructing trachea with different materials, including electrospun polycaprolactone [12, 13], freeze-dried gelatin sponge [14, 15], 3D printed tubular shape using poly(ε-caprolactone) diol and polyethylene butylene adipate diol [16].

Decellularization techniques are increasingly explored for creating tissue regeneration scaffolds. This process involves removing all cellular contents from donor tissue while preserving the extracellular matrix (ECM). The resulting decellularized ECM serves as an effective scaffold in tissue engineering, providing a microenvironment for the coherent development of patient-derived cells [17–19]. This approach offers potential advantages, including low risk of immune rejection, structural integrity, and biocompatibility [20–23]. Numerous studies have investigated the feasibility of decellularized tissues and organs for applications such as heart, lung, liver, kidney, pancreas, skin, bone, and cartilage replacement [20, 24–29]. The trachea, with its intricate structure, features ciliated epithelial cells and goblet cells on the lumen side, aiding in mucus and debris clearance [30–32]. C-shaped cartilage rings support the tubular shape and prevent airway collapse [2, 33]. Besides, the trachea hosts blood vessels and nerves. Decellularized trachea (dTrachea) has been clinically used with long-term monitoring, involving

seeding autologous cells [34–36]. Many studies have either overlooked the reconstruction of cartilage rings necessary for maintaining the tubular shape of decellularized trachea or have not addressed the replacement of non-viable cartilage rings after the decellularization process [34–40].

The anatomical complexity of the trachea requires the use of a decellularized tracheal tissue to investigate its microarchitecture for cell attachment, biocompatibility, and potential use as a tracheal replacement. Canine trachea, due to its similarity in mechanical and dimensional features compared to the human trachea [41], was chosen as a tissue model for practicing the decellularization protocol and preparing the hydrogel due to its mechanical and dimensional resemblance to human tracheas. This choice allows us to refine our protocols for potential future application in humans. We are investigating the feasibility of creating two distinct types of cell carriers. This preference for canine models lays the foundation for extending our methods to the decellularization of human trachea and the generation of hydrogel from human decellularized trachea. Many investigations have been studied the effects of decellularized trachea scaffolds in human, porcine, and rabbit models [40, 42, 43]. However, no attempts have been made to investigate the application of decellularized trachea scaffolds in canines.

This study aimed to prepare ECM-rich cell carriers from the decellularized canine trachea for human epithelial cell seeding, hMSC encapsulating, and human umbilical vein endothelial cell (HUVEC) supporting. An underlying hypothesis of this study is that the decellularized tissue contains a range of ECM constituents, growth factors, and cytokines to provide a microenvironment for newly seeded cells without cytotoxicity. Our study focused on the preparation of ECM-rich biomaterials and assessing their cytotoxicity. Short-term cell culture experiments were conducted for both cell-carrier formats. Re-epithelialization was observed on the lumen side of the decellularized tracheal scaffold. Viability of hMSCs encapsulated in the hydrogel and formation of capillary-like structures by HUVECs were also investigated. Long-term culture for epithelial differentiation and cartilage tissue formation was not conducted. This study serves as a proof-of-concept, demonstrating that decellularized trachea supports epithelial cell viability and dECM hydrogel sustains human mesenchymal stem cell viability. This crucial step lays the groundwork for our next study, which will involve long-term culture. Overall, our work serves as a valuable resource for future studies focusing on the ciliated epithelial lining on the lumen side and the development of cartilage rings, both of which are crucial features for a functional trachea.

Materials and Methods

Chemicals and Reagents

Phosphate buffered saline powder, Sodium deoxycholate, DNase I (750KU), and Triton X-100 were purchased from Sigma-Aldrich (St. Louis, MO). Antibiotic-antimycotic solution (100X) and Ambion® RNase I (100 U/µL) were purchased from Gibco and Invitrogen (Thermo Fisher Scientific Inc., PA, USA), respectively. Proteinase K and Papain were purchased from Worthington biochemical corporation (Lakewood, NJ). The airway epithelial cell growth medium was purchased from Promocell GmbH, Heidelberg, Germany.

Harvesting Canine Tracheal Tissue

Canine tracheae ($n = 6$) were harvested under sterile conditions from canine donors kindly supported by the Faculty of Veterinary Science, Chulalongkorn University, Thailand. Animal surgery and husbandry were performed by the Thailand guidelines on the use of experimental animals (ANIMALS FOR SCIENTIFIC PURPOSES ACT, B.E. 2558 (A.D. 2015). This study was approved by the Institutional Animal Care and Use Committee (IACUC) of Chulalongkorn University (No. 2231001). The tracheae were immediately rinsed in 40 mL of phosphate-buffered saline (PBS) containing 3% antibiotic–antimycotic.

Preparation of Decellularized Canine Trachea (dTrachea)

Tracheae were frozen at $-80\ °C$ prior to decellularization using chemical and physical techniques, namely vacuum-assisted decellularization (VAD) method [43–45]. Briefly, tracheae were thawed for 24 h at 4 °C, removed surrounding tissue, and washed with 1xPBS for 24 h at 4 °C on a rocker. For decellularization, all steps were taken place in a vacuum chamber together with detergent and enzymatic treatment. All solutions were supplemented with 1% antibiotic-antimycotic. The tracheae were incubated in a detergent solution containing 0.25% sodium deoxycholate and 0.25% Triton X-100 in PBS for 24 h at 37 °C on a rocker. Afterward, the tracheae were rinsed twice in DI water type II for 4 h and incubated for another 44 h in DI water type II at 4 °C. At enzymatic treatment, the tissues were incubated in 2 kU/ml DNase I and 4 U/ml RNase I at 37 °C for 24 h and washed with DI water type II at 4 °C for 24 h. This enzymatic treatment step was repeated one more time. Finally, tracheae were washed with DI water type
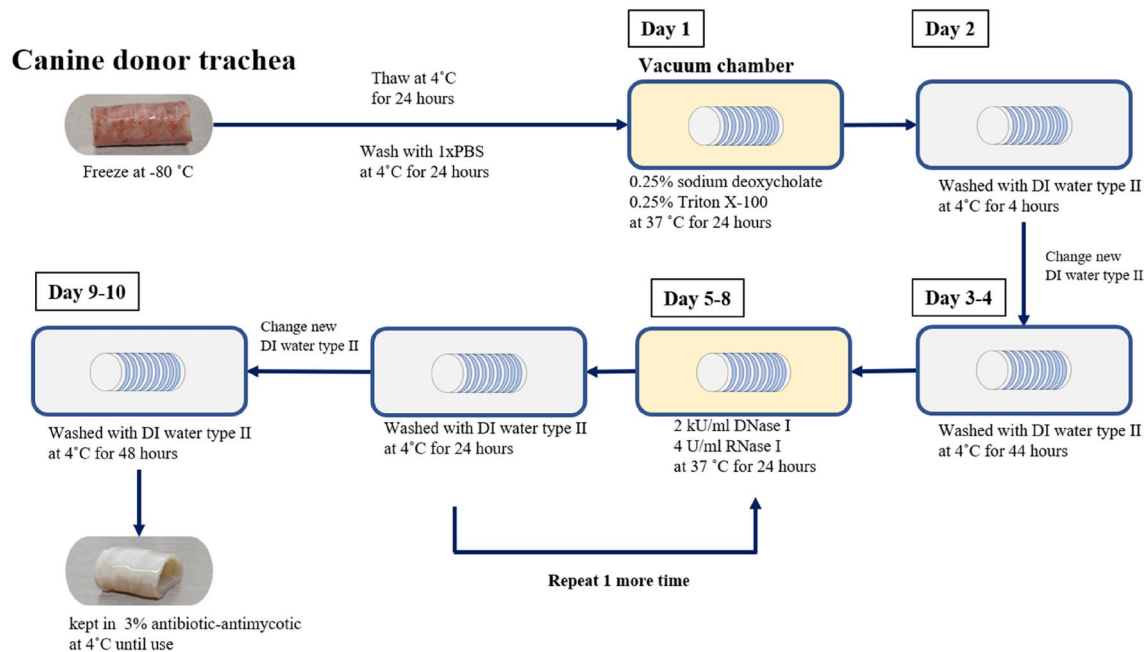
Fig. 1 Vacuum-assisted decellularization of the trachea The canine trachea was washed in a vacuum chamber for 10 days by changing different solutions. On day 1, the trachea was incubated in a detergent solution and washed with DI water type II. On days 5–8, nucleic acid materials of the trachea was removed in DNase I and RNase I solutions. The decellularized trachea was kept in a 3% antibiotic–antimycotic solution at 4 °C until use.

II for 48 h and kept in 1xPBS containing 3% antibiotic-antimycotic at 4 °C until use (Fig. 1).

Histology, Immunohistochemistry, and Immunofluorescence

The decellularized trachea (dTrachea) was fixed with 4% paraformaldehyde, embedded in paraffin, and sectioned to 3 μm thick. The sections were stained with hematoxylin and eosin (H&E). The extracellular matrix components (collagen, sGAG, elastin, muscle, mucin and fibrin) were examined using Movat pentachrome stain kit (Modified Russell-Movat). The presence of a major histocompatibility complex (MHC) marker was detected by monoclonal mouse anti-human HLA-DP, DQ, DR antibody [CR3/43] at 1:100 dilution (M0775, Dako). Horse anti-mouse IgG antibody (H+L) biotinylated at 1:200 dilution (BA-2000-1.5, Vector Laboratories) was used as secondary antibody. Then, sections were incubated with ImmPACT DAB substrate kit (Vector Laboratories) according to the manufacturer's instructions and finally counterstained with hematoxylin.

For laminin and fibronectin detection, the dTracheae ($n=3$) were fixed with Cryo-gel (Leica Biosystems, USA), incubated with 2.5% horse serum for 1 h at room temperature, and washed with 1xPBS for 3 min. Next, the sections were incubated with primary antibody at 1:200 dilution (rabbit polyclonal antibody to laminin; ab11575 or anti-fibronectin antibody [IST-9] - BSA and Azide free; ab6328) for overnight at 4 °C. The sections were washed with 1xPBS for 3 min and incubated with secondary antibody at 1:200 dilution (goat polyclonal antibody to rabbit IgG (IR, Texas red; ab6719) or goat polyclonal antibody to mouse IgG (FITC; ab97239) for 2 h in the dark at room temperature. Finally, the samples were washed with 1xPBS and stained with DAPI (Fluroshiled Mounting medium with DAPI; ab104139). All antibodies are from Abcam company (Cambridge, United Kingdom). All sections were observed under a microscope (Nikon; ECLIPSE: Ti-U, Tokyo, Japan) and analyzed using the NIS-Elements BR imaging software (vD4.10.02; Nikon Instruments, NY, USA).

Mechanical Assessment

Compression and tensile tests were performed using the Universal testing machine (Hounsfield-H10KM, USA). Length and wall thickness of unwashed and dTracheae were recorded (Table S1). The dTracheae were compressed at a speed of 5 mm/min in the anterior-posterior direction until the diameter decreased to 50% of the starting diameter in dry condition, at 25 °C approximately for 30 minutes. Young's Modulus was calculated as the slope of a stress and strain curves using ASTM C 165 compressive properties software (Tinius Olsen, Kongsberg, Norway). For tensile testing, two fixtures were placed inside the lumen side of trachea. Each

sample underwent tensile testing at a rate of 50 mm/min. The tensile strength, ultimate tensile strength, and % elongation were analyzed using ASTM D 882 Simplified Tensile & Break software (Tinius Olsen, Kongsberg, Norway). The unwashed tracheae were used as control.

Preparation of Extracellular Matrix-Derived Solution (dECM Solution)

The dTracheae were cut into small pieces (8 mm) and washed in DI type II containing 3% antibiotic/antimycotic. The samples were snap frozen at −80 °C, freeze-dried for 2 days, and milled using a grinder machine. The dried tissue was sterilized by gamma irradiation (15 kGy for 5 h) and stored at −80 °C until use. Canine tracheal tissue was enzymatically digested as previously described [46, 47]. Decellularized canine tracheae weighed 20 mg and put into 10 ml of 0.5 M acetic acid (pH 3.0) with 22 mg of pepsin (627U/mg, P7000-100G; Sigma) at a final solute concentration of 1.1 mg pepsin per 1 mg of tissue. The peptic digestion was performed at room temperature under constant agitation. The digested samples were collected at 4, 12, 24, 48, and 72 h, and centrifuged at 10,000 rpm for 15 minutes to remove undigested tissues. Supernatant was collected and dialyzed against 0.01 M acetic acid at 4 °C (Snakeskin MWCO 3500, Thermo Fisher scientific, USA) for 2 days, as modified from published protocols [47]. Afterward, the dialyzed solution was collected and kept at 4 °C (Fig. S1).

Biochemical Quantification of dTrachea and dECM Solution

The dTrachea and dECM solution were digested in 1 ml of proteinase K buffer (1 mg/ml Proteinase K and 0.88 mg/ml papain), incubated at 60 °C overnight and centrifuged at 6000 rpm at 4 °C for 20 min. The supernatant was transferred to new microcentrifuge tubes. The DNA content was measured using the Quant-iT PicoGreen® dsDNA Assay Kit (Life Technologies, Grand Island, NY). Sulfated glycosaminoglycan (sGAG) content was determined by DMMB dye-binding assay, and the total collagen contents were determined by Ortho-hydroxyproline (OHP) colorimetric assay with a reaction of chloramine T and dimethyl-amino benzaldehyde [48]. Additionally, laminin (ab119572), and fibronectin (ab108849) were performed using ELISA kits (Abcam, Cambridge, United Kingdom) according to the manufacturer's instructions.

Characterization of the dECM Solution by Western Blot Analysis

The 25 μL of dECM solution (5 μg of total protein) were loaded on a 4–15% Mini-Protein TGX gels (Bio-rad

Laboratories, California, USA). Electrophoresis was conducted at 120 V for 65 minutes. Then, proteins on SDS-PAGE were transferred to an Immun-Blot PVDF membrane (Bio-rad Laboratories, California, USA) at 4 °C, 100 V for 2 h. The membrane was blocked with 3% BSA in 0.1% Tris-buffered saline with 0.1% Tween® 20 Detergent (TBST) at 4 °C for overnight with agitation. The membrane was rinsed with 0.1% TBST for 3 times, incubated with rabbit polyclonal antibody collagen type II (ab34712, Abcam) at dilution of 1:5000 in 3% BSA containing 0.1% TBST at 4 °C for 2 h, and rinsed with 0.1% TBST for 3 times. The membrane was incubated with goat anti-rabbit IgG H&L HRP (1:5000, ab205718, Abcam) for 2 h and 4 °C and rinsed with 0.1% TBST for 3 times. The Western blotting detection reagent (Amersham ECL Prime, GE healthcare) was added on the membrane and the signals were detected by Visionworks software on the UVP GelStudio imaging system (Analytik Jena GmbH, USA).

Gelation Kinetics of the dECM Solution

Gelation of the dECM solution was determined by turbidimetric gelation kinetics [46, 49]. The dECM solution obtained from method 2.6 was filtered sterile, chilled on ice, and adjusted to pH 7.4 by cold 10 N NaOH to deactivate pepsin activity. Then dECM solution was transferred to a 37 °C incubator to initiate gelation. The sterile, neutralized dECM solution from method 2.6 The dECM solution (50 μL) was incubated at 37 °C and recorded the absorbance every 5 min for 60 min at 405 nm by Microplate reader (Varioskan LUX Multimode Reader, Thermo Fisher Scientific, UK). The normalized absorbance (NA) was calculated at each digestion time point using Eq. (1)

$$NA = (A_t - A_0)/(A_{max} - A_0) \tag{1}$$

where A_t is the absorbance at time point t, A_0 is the initial time point t_0, and A_{max} is the maximum absorbance value.

Morphological Assessment of dECM Hydrogel by SEM

The dECM hydrogels were fixed in 2.5% glutaraldehyde in 1xPBS at 4 °C overnight and prepared as previously descript in method 8. The dried hydrogel constructs were sputter-coated with Gold (Au) and analyzed by a scanning electron microscope and energy dispersive x-ray spectrometer at ×5000 magnification (JSM-IT500HR, JEOL Group Companies, Japan). The 3 fields of views were selected and measured diameter of 12 fibers [46]. by Image J software (National Institutes of Health, NIH). For the total number of branching fibers, the branching points on 12 fibers were

recorded and divided by the area of the field of views (6.25 μm^2) to obtain [interconnections/μm^2].

Re-epithelization of dTrachea

Cell Culture and Cell Seeding

Primary human bronchial epithelial cells (HBEpC, C-12640; Promocell GmbH, Heidelberg, Germany) were expanded in airway epithelial cell growth medium and cultured in 5% CO_2 at 37 °C, with medium change every 2 days. The 1×10^6 HBEpC in 200 µl of the growth medium were seeded directly on the lumina side of dTrachea disks, 5 mm in diameter ($n=3$). The constructs were transferred into a 96-well plate (NUNC, Fisher Scientific GTF, Sweden), coating with 2% agarose gel and kept in 5% CO_2 at 37 °C overnight to allow cell attachment and cultured for 3 and 14 days in growth medium. Non-seeded decellularized trachea served as a control group.

LIVE/DEAD® Staining

Cytotoxicity of dTracheae were assessed using LIVE/DEAD® Viability/Cytotoxicity Kit (Thermo Fisher Scientific). Briefly, the cell-seeded constructs at day 3 and were incubated in 200 µl of 1xPBS containing 2 µM Calcein AM and 4 µM Ethidium homodimer-1 (EthD-1) for 45 min at 37 °C, 5% CO_2. The constructs were washed two times with 1xPBS and visualized under fluorescence microscope. Subsequently, all constructs were collected to analyze DNA content by Quant-iT PicoGreen® dsDNA Assay.

Micromorphological Assessment of Re-epithelization

To evaluate micromorphological of the cell-seeded adhesion, constructs were fixed after day 3 with 2.5% glutaraldehyde in 1xPBS at 4 °C overnight, washed with 1xPBS for 3 times for 10 minutes each at room temperature and rinsed with DI water. The constructs were dehydrated in graded ethanol series from 30 to 100% ethanol and evaporated using a critical point dryer (Leica EM CPD300). The dry constructs were sputter-coated with Gold (Au) (BALZERS SCD 040) and analyzed by a scanning electron microscope and energy-dispersive X-ray spectrometer at ×10,000 and ×3000 magnification (JSM-IT500HR, JEOL Group Companies, Japan).

Histological Analysis

Re-epithelialization on dTrachea at day 3 and 14 were fixed with 4% paraformaldehyde, embedded in paraffin, and sectioned to 3 µm thick. The sections were stained with hematoxylin and eosin (H&E).

Encapsulation of hMSCs in dECM Hydrogel

Cytotoxicity of dECM Hydrogel

The 400 µL of dECM solutions after neutralization, prepared from peptic digestion of dTrachea at 24 h, 48 h, and 72 h in method 2.6, were added into a 24-well plate and incubated at 37 °C for 1 hour to allow gelation. According to ISO standard 10993-5:2009, the resulting dECM hydrogels were incubated with 2 ml of serum free alpha-MEM medium for 24 h to prepare the dECM hydrogel's extracts. The hMSCs (hMSC, C-12972; Promocell GmbH, Heidelberg, Germany) were seeded at a density of 30,000 cells /cm^2 into 96-well plate and incubated at 37 °C, 5% CO_2 for 24 h to allow cell attachment. The hMSC medium (alpha-MEM medium containing 4% FBS, 1% antibiotic-antimycotic, 1% Glutamax, 1% Hepes buffer, and 1 ng/mL recombinant human basic fibroblast growth factor; bFGF) was removed and replaced by with the dECM hydrogel's extract solution. The metabolic activity of cells was assessed using PrestoBlue™ according to the manufacturer's instructions. The hMSC medium and 100% DMSO were used as positive and negative controls, respectively.

Encapsulation of hMSCs in dECM Hydrogel

The hMSCs 100,000 cells were mixed with 500 µl of dECM solution, transferred to 24-well plate, incubated at 37 °C, 5% CO_2 for 1 h to allow gelation, and cultured for 3 days in hMSC medium. The cell-seeded hydrogels were tested for cell viability using the LIVE/DEAD® assay (see section 2.11.1.2) and visualized by a confocal microscope Zeiss LSM 800 (ZEISS, Oberkochen, Germany).

HUVEC Viability and Tube Formation Assay on dECM Hydrogel

Human umbilical vein endothelial cells (HUVECs) were obtained from PromoCell (Heidelberg, Germany) to investigate the formation of capillary-like structures in vitro. HUVECs were grown in Endothelial Cell Growth Media-2 (EGM-2, PromoCell) and maintained at 37 °C, 5% CO_2 and 95% humidified air. For each well in a 96-well plate, 20,000 cells were seeded onto 50 µl dECM hydrogels, which were prepared from 72-h peptic digestion. The HUVEC-hydrogels were inculcated at 37 °C with 5% CO_2 and visualized under light microscopy (SA115B-05V, Olympus, China) at 0, 4, and 24 h. HUVEC viability was determined at 24 h using LIVE/DEAD® staining, visualized under fluorescence microscopy (Nikon; ECLIPSE: T*i*-U, Tokyo, Japan), and analyzed using the NIS-Elements BR imaging software (vD4.10.02; Nikon Instruments, NY, USA). Matrigel®, and fibrin gel [50] were used as control hydrogels.

Statistical Analysis

Statistical analysis was performed using GraphPad Prism 9.0 software (La Jolla, CA). Unpaired t test was used for mechanical testing and biochemical content, respectively. ELISA assay of ECM contents was used two-way ANOVA analysis. Bonferroni post hoc analysis was performed with $\alpha = 0.05$ to consider statistical significance. All data were expressed as mean $\pm$ standard deviation of $n = 3$ to 4 samples per group.

Results

Appearance of dTrachea

The tracheal tissue exhibited a white appearance after decellularization for 10 days (Fig. 1). In H&E staining, mucosa and submucosa layers of the unwashed control trachea showed the pseudostratified ciliated epithelial cells, glands, and smooth muscle, while cells were removed in a dTrachea group (Fig. 2a). The cartilage layer of the unwashed group showed intact chondrocytes surrounded by an ECM (Fig. 2a). The dTrachea group showed similar signal of muscle and fibrin (red) to the unwashed group in Pentachrome staining (Fig. 2b). Collagen staining (yellow) was detected in cartilage layer. Glycosaminoglycan depletion (purple) in cartilage layer was observed in dTrachea group. The presence of MHC class II was clearly detected in the submucosal layers in the unwashed control group, whereas the signal did not detect in cartilage layer (Fig. 2c). Interestingly, MHC class II was not observed in cartilage layer both control and dTrachea groups (Fig. 2c). Moreover, decellularization could preserve laminin and fibronectin, demonstrated by immunofluorescent staining in Fig. 3a and b.

Biomechanical Properties of dTrachea

Decellularization preserved mechanical properties of canine trachea (Table 1). In the compressive test, the dTrachea did not show a significant difference ($P > 0.05$) in Young's modulus ($P = 0.1092$), stress ($P = 0.4246$), and strain ($P = 0.6385$) compared to unwashed control trachea (Table 1, Table S2). Moreover, dTrachea group could return to its original shape after removal of loads. For tensile test, the tensile strength ($P = 0.8545$), ultimate tensile strength ($P = 0.8545$), and percent elongation ($P = 0.9644$) did not show significant differences between dTrachea and control group (Table 1, Table S3).

Characterization and Gelation of the dECM Solution

The dECM solution obtained from peptic digestion was examined by SDS-PAGE and Western blot analysis. Protein bands of the digested trachea sized around 140 kDa showed stronger signals when peptic digestion times increased from 4 to 72 h (Fig. 4a). Collagen type II was detected by Western blot analysis at 140 kDa and 270 kDa for monomeric and dimeric structures, respectively (Fig. 4b). The dECM solution obtained from peptic digestion for 72 h maintained the highest absorbance value of 0.7 at 405 nm for 60 min, whereas 4 h and 12 h groups exhibited more clear solution and showed similar absorbance values around 0.4 (Fig. 4c). The dECM solutions obtained from peptic digestion for 4 and 12 h exhibited temporary gelation for 20 min, as demonstrated by a decrease in absorbance, while the 24-, 48- and 72-h peptic digestion groups could form hydrogels entire time-course of experiment for 60 min (Fig. 4d).

Biochemical Analysis of dTrachea and dECM Solution

The DNA contents of dTrachea (2.46 ± 0.33 %DNA/ wet weight) and dECM solution (1.16 ± 0.14 %DNA/ wet weight) were significantly decreased compared with those of unwashed control trachea ($P < 0.0001$) (Fig. 5a, Table S4). The ECM components, such as glycosaminoglycan (sGAG), collagen, laminin, and fibronectin, of dTrachea group, were not significantly reduced by decellularization ($P < 0.05$) (Fig. 5b–e, Table S4). Interestingly, dECM solution significantly decreased in sGAG ($P = 0.0069$), collagen ($P = 0.0018$), and fibronectin ($P = 0.0025$) compared to unwashed control group; however, no significant difference in laminin ($P = 0.761$) between dECM solution and unwashed group was found. (Fig. 5b–e, Table S4).

Microarchitecture of dECM Hydrogel

The SEM image of dECM hydrogels, prepared from peptic digestion of dTrachea for 24 h, showed more debris compared to longer digestion groups (Fig. 6a). Interestingly, the dECM hydrogel of the 72-h digestion group exhibited clear and intact extracellular matrix fibers with diameter of 0.085 ± 0.005 μm, which were significant smaller than those of 24-h group (0.168 ± 0.015 μm) and 48-h group (0.131 ± 0.010 μm). The interconnectivity of fibers increased when decellularized tissues exposed to longer peptic digestion times (Fig. 6b). The 72-h group showed the highest interconnectivity of ECM fibers of 0.840 ± 0.182 intersection points/μm^2 (Fig. 6d, Table S5).
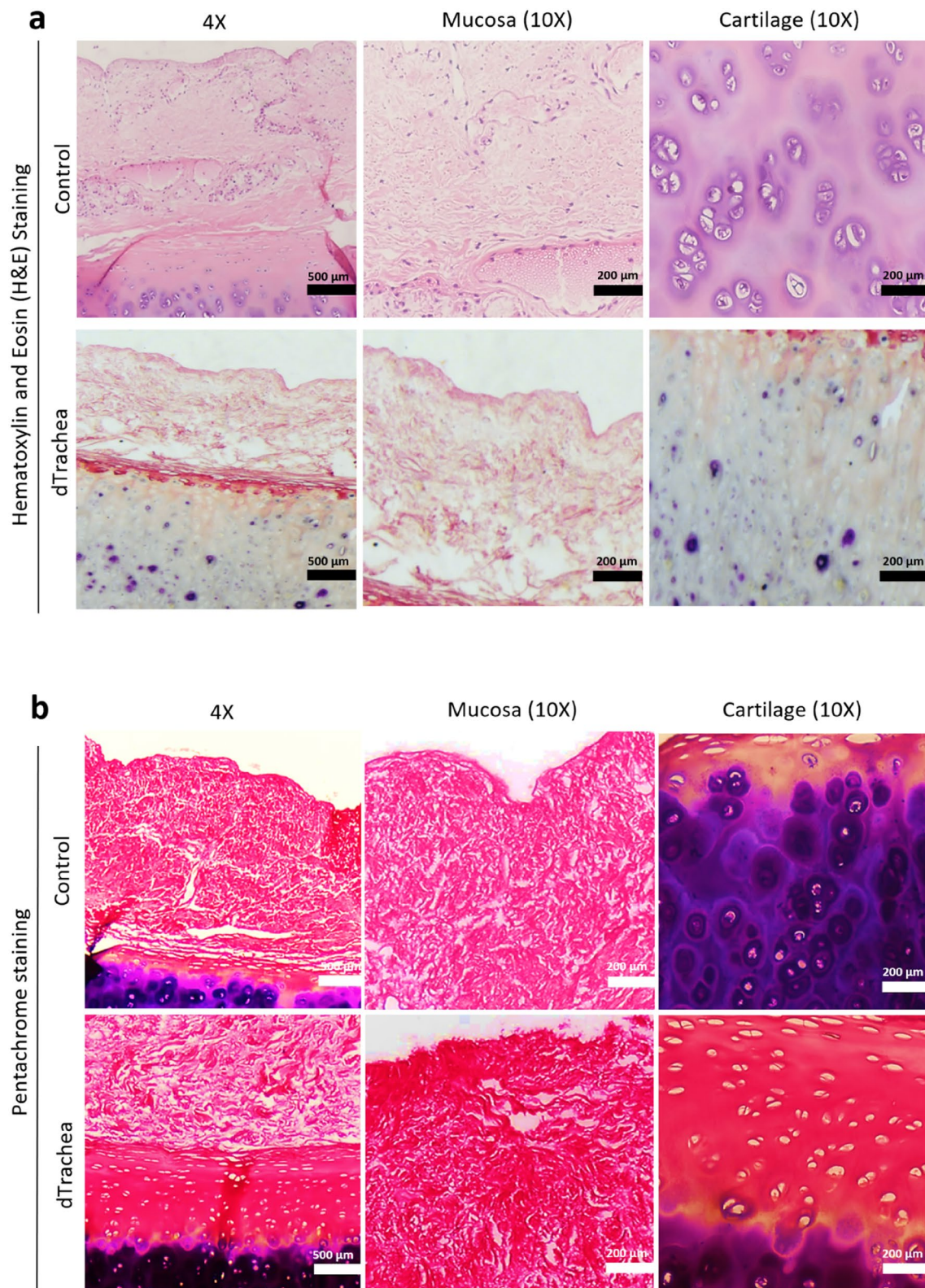
Fig. 2 Histological evaluation of the decellularized trachea. **a** Hematoxylin and eosin staining. **b** Pentachrome staining. **c** Immunostaining of MHC-II. Control, unwashed trachea; dTrachea, decellularized trachea
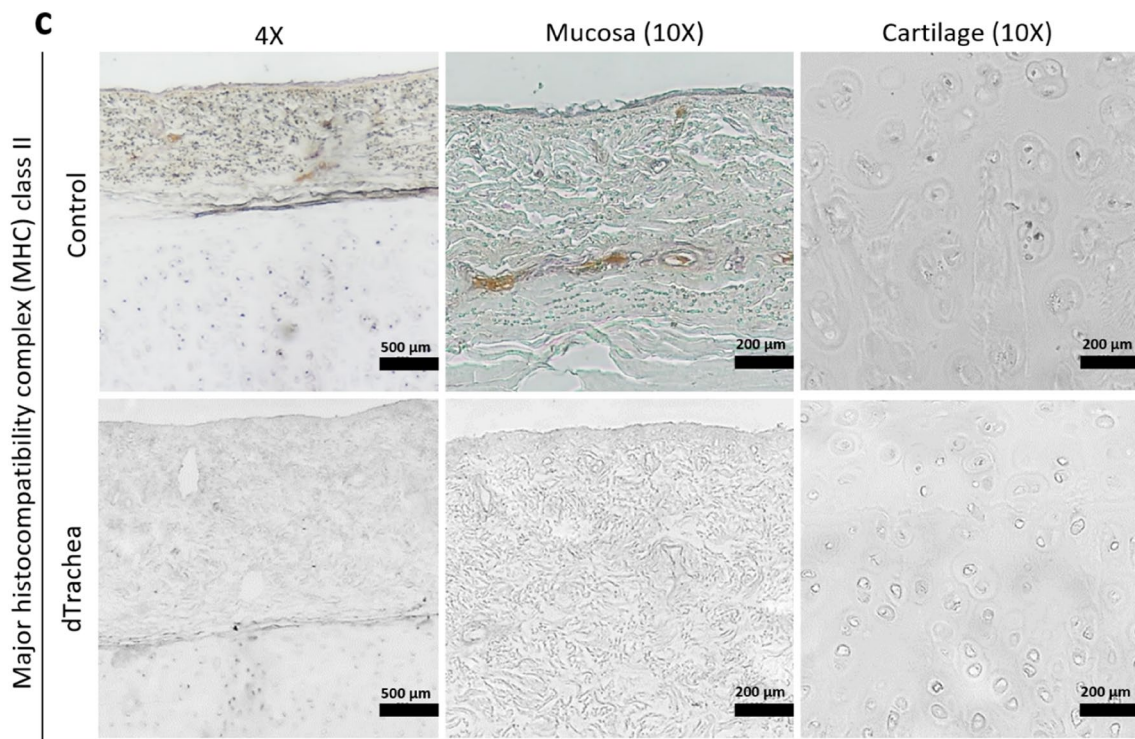
Fig. 2 (continued)

Application of ECM-Rich Cell Carriers

Re-epithelialization of dTrachea

Epithelial cells were removed by decellularization. Newly seeded HBEpC exhibited excellent cell viability after 3 days post-seeding on the luminal surface of the dTrachea (Fig. 7a). The microarchitecture of dTrachea showed a mesh-like structure and an intricate ECM network, allowing the HBEpCs attachment on mucosa layer of the luminal surface (Fig. 7b). DNA quantification confirmed the presence of HBEpCs on the decellularized scaffold constructs (Fig. 7c). In long-term culture, epithelial cells were further cultured to 14 days. The epithelial cells clearly attached on mucosa layer and infiltrated into the submucosal layers (Fig. 7d).

Assessment of Cell Encapsulation in dECM Hydrogel

The effects of dECM hydrogels on hMSCs viability were evaluated using PrestoBlue™ assay and LIVE/DEAD® assay. The viability percentages of hMSCs culture in extracted media of all dECM hydrogels for 24 h were higher than 70% (Fig. 8a), indicating non-cytotoxicity of dECM hydrogels against hMSCs. At 3 days (72 h) post-encapsulation, hMSCs exhibited excellent cell viability and showed homogeneous distribution in all dECM hydrogels (Fig. 8b). We adjusted components of the dECM hydrogel by

incorporating fibrin to improve injectability (Fig. S2). This dECM-fibrin hydrogel mixed with hMSCs was intended to be used for constructing cartilage rings, located on the outer surface of the dTrachea.

Viability Analysis and Tube Formation Assay of HUVECs

Our results demonstrated that HUVECs formed tube-like structures on Matrigel® by 4 h, whereas the cells distributed evenly as a monolayer on fibrin and dECM hydrogels (Fig. 8c). By 24 h, HUVECs showed excellent viability on fibrin gel and dECM hydrogel; however, the tube-like structures of HUVECs on Matrigel® group became detached.

Discussion

Tracheal tissue engineering offers the potential to replace damaged tracheae by combining airway cells into a tubular-shaped scaffold. Creating hollow structures for cell culture is challenging because they must be strong enough to not collapse or be sutured and must provide a suitable environment for cell attachment and growth.

In this study, the dTrachea retained its structural integrity, as demonstrated by the similar biomechanical properties of the trachea to the unwashed trachea and mimicked a microenvironment, allowing the attachment of epithelial
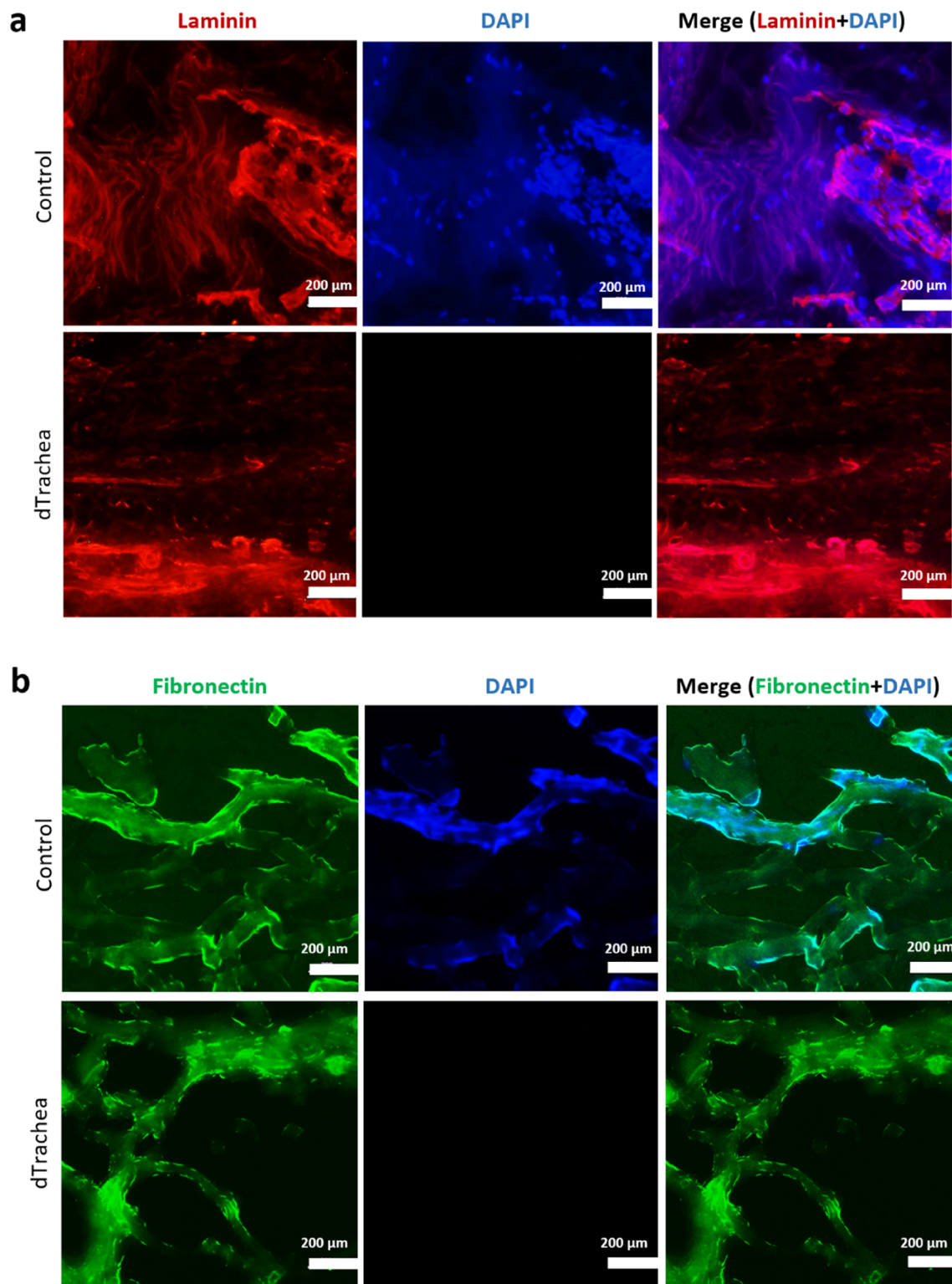
Fig. 3 Immunofluorescence detection of laminin and fibronectin in decellularized trachea. **a** laminin and **b** fibronectin in decellularized trachea (dTrachea) compared with the unwashed trachea (Control). Scale bar = 200 μm.

Table 1 Mechanical parameters of the unwashed and decellularized trachea

Mechanical test		Unwashed trachea (control)	dTrachea	P value
Compressive test	Young's modulus (kPa)	1124.76 ± 81.42	1030.43 ± 58.66	0.1092^{ns}
	Stress (kPa)	146.78 ± 28.19	131.86 ± 20.47	0.4246^{ns}
	% Strain	18.36 ± 7.84	15.91 ± 6.06	0.6385^{ns}
Tensile test	Tensile strength (kPa)	3920.0 ± 817.06	3809.0 ± 822.54	0.8545^{ns}
	Ultimate tensile strength (kPa)	212675.00 ± 60607.67	210700.00 ± 30664.75	0.9555^{ns}
	% Elongation	43.50 ± 7.38	43.23 ± 8.96	0.9644^{ns}

Data were expressed as mean $\pm$ standard deviation ($n = 4$)

NS no significant difference

$*P < 0.05$

cells. The canine trachea was chosen as a tissue model for implementing the decellularization protocol and preparing the hydrogel. This choice of model enables us to enhance and fine-tune our protocols for potential future applications in human contexts. The limitation of the canine model is attributed to the unavailability of commercially produced antibodies, prompting the use of the canine trachea as a model. Looking ahead to translate our findings to human applications, our future plans involve working on donated human cadaveric trachea.

The dTrachea was prepared by washing the canine trachea under vacuum conditions with detergent and nuclease enzymes [43, 51, 52] to remove cellular components, such as proteins, lipids, and nucleic acids, which are major triggers of an immune response, resulting in complications with organ rejection [23]. In H&E staining and DNA quantification (Figs. 2a and 4b), cells were not detected in the submucosal layers of the dTrachea. However, traces of cellular components were observed in the cavities (lacunae) at the cartilage layer (Fig. 2a).

The decellularization protocol in conjunction with vacuum efficiently removed MHC class II while preserving the ECM, as demonstrated by a non-significant decrease in sGAG, collagen, laminin, and fibronectin compared with the unwashed control group. These ECMs play various roles in tissue development, including providing a physical structure for cells, acting as a barrier between different tissues, aiding in cell-to-cell communication and guidance during development, storing growth factors and cytokines necessary for cellular survival and proliferation, facilitating nutrient transport within tissue compartments, and regulating gene expression patterns associated with specific cell types or functions [20, 24, 29, 49, 53, 54]. Excessive removal of the ECM could inhibit cell attachment, as demonstrated by a decrease in epithelial cell attachment in a decellularized lung tissue with low GAG content [55]. Primary HBEpCs distributed evenly on the mucosa layer and nicely attached to the ECM networks of the dTrachea. Re-epithelialization of a donor's dTrachea is a crucial step in cell-based tracheal reconstruction to help restore the normal structure and function of airway tissue [34] and increases tracheal strength and flexibility, which makes it more suitable for implantation in patients with damaged airways [37].
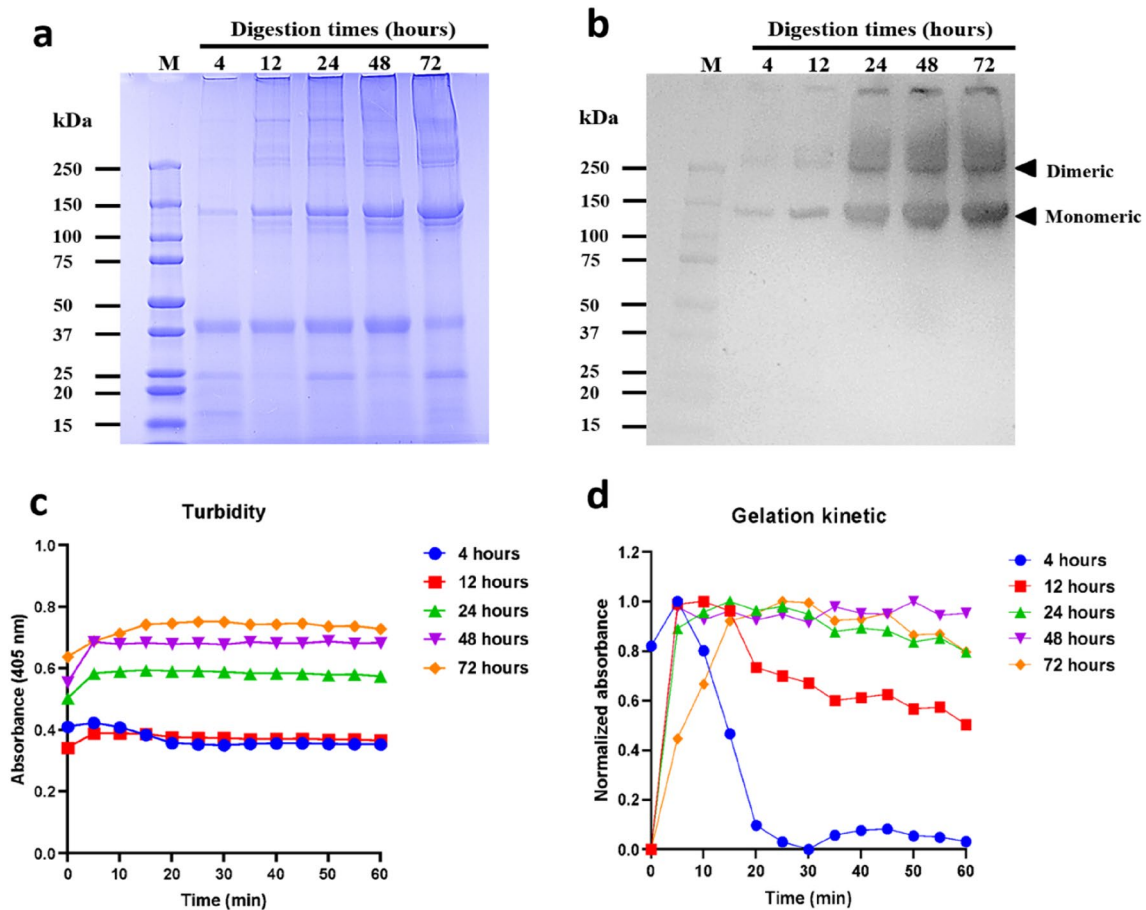
Fig. 4 Characterization of the extracellular matrix-derived solution (dECM solution). **a** SDS-PAGE of decellularized trachea digested by pepsin for 4, 12, 24, 48 and 72 h. **b** Detection of collagen type II by Western blot analysis. **c** An increase in turbidity of dECM solution at different peptic digestion time. **d** Gelation kinetics of dECM solution

dTrachea without seeding with epithelial cells were also reported as an effective platform for epithelial cell infiltration from healthy segments of the trachea [37], and for enhancing the healing process or reducing inflammation response [42, 56]. In addition, these scaffolds could be used as a potential delivery system for drugs or therapeutic agents due to their porous structure, which allows for controlled release over time [24].

It is important to note that dTrachea is stripped of native cellular components; as a result, it does not have any inherent ability to self-repair or regenerate. Therefore, we seeded primary HBEpCs on the lumen side of the dTrachea, which could be beneficial for tracheal tissue reconstruction and promote long-term tissue regeneration. The newly seeded HBEpCs attached and migrated to submucosal layers of dTrachea, highlighting their potential for re-establishing a

functional mucosal lining in tracheal reconstruction. Moreover, non-seeded dTrachea was more likely to experience degradation over time [39, 56]. We have proved that ECM-rich dTrachea did not show toxicity, and it provided attachment sites for epithelial cells, which could be further differentiated to ciliated pseudostratified columnar epithelial cells when induced by growth factors, including epidermal growth factor (EGF), and fibroblast growth factor (FGF) [57, 58].

The underlying hypothesis of using dTrachea as a scaffold in this study is that a range of biochemical niche secreted by the resident cells of tracheal tissue will provide microenvironment for newly seeded cells. The versatility of the dTrachea in airway regenerative medicine was explored using tracheal ECM to create two types of cell-carriers for two distinct cell types: epithelial cells and hMSCs. Besides investigation of biological function of an intact dTrachea
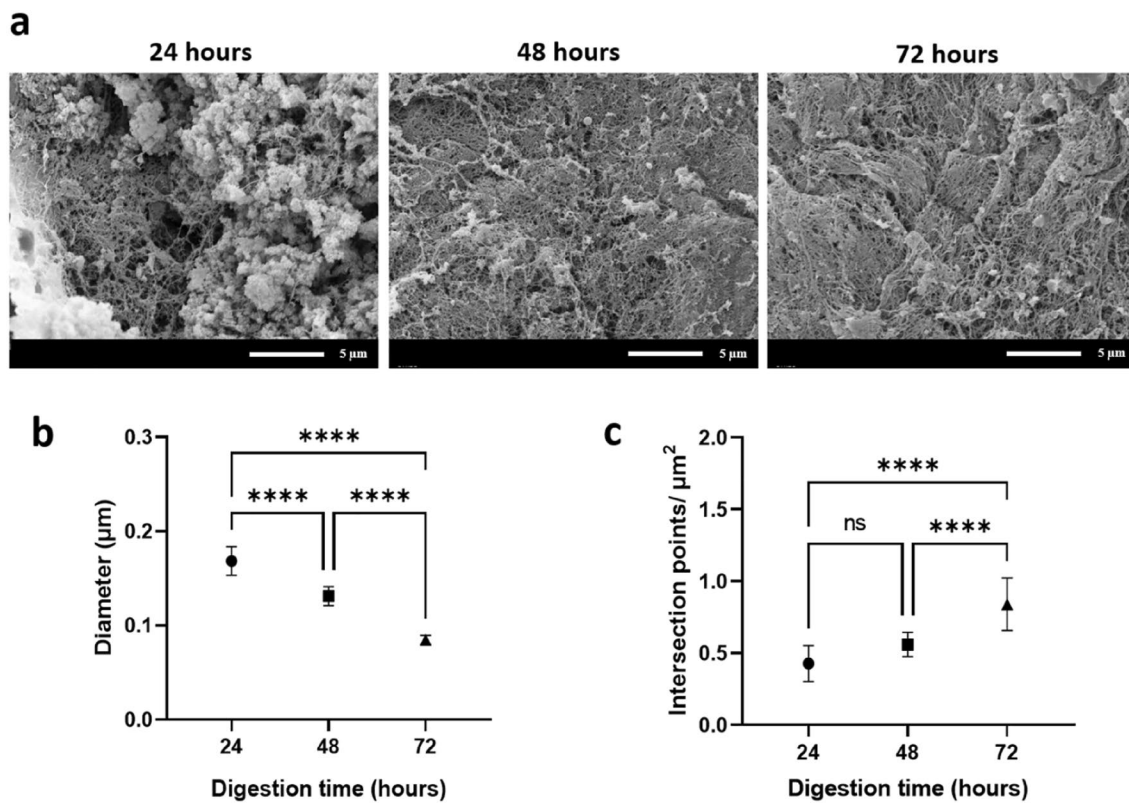
Fig. 5 DNA content and extracellular matrix composition of the decellularized trachea. Decellularized tracheal tissues were analyzed for **a** DNA content, **b** sGAG contents, **d** collagen content, **f** laminin content, and **e** fibronectin content ($n=4$). ns, not significant, **$P<0.01$, ***$P<0.001$, and ****$P<0.0001$. Control, unwashed trachea; dTrachea, decellularized trachea; dECM solution, extracellular matrix-derived solution

to support cell attachment, the dTrachea was prepared in a liquid form (dECM solution) and were induced to form a hydrogel (dECM hydrogel). The resulting ECM-rich hydrogel is intended to be used for encapsulating hMSCs, which could be differentiated to chondrocytes found in cartilage rings of trachea. Further investigations are necessary to understand if bioinductive properties of the dECM hydrogel can support chondrogenic differentiation of hMSCs. The ECM hydrogel in this study is a collagen-based self-assembly with other proteins which was neutralized to physiological pH of 7.4 and allowed to form hydrogel at 37 °C [46].

Interestingly, the dECM solution showed a significant decrease in sGAG, collagen, and fibronectin compared

with the intact dTrachea. The lower ECM content in the dECM solution could be explained by the breakdown of peptide-based extracellular matrix during homogenization and peptic digestion, resulting in a partial loss of ECM content from the intact dTrachea. The major function of pepsin is to cleave the telopeptide of the collagen triple helix structure, allowing collagen fibril to unravel [59]. Although an increase in pepsin digestion time helped remove tissue debris and allowed collagen fibrils to release more, peptic over digestion is highly concerning, as bioactive cryptic molecules will be lost. At 48 and 72 h of trachea digestion, the dECM solution was cloudy and spontaneously formed gel at physiological pH [53]. However,

Fig. 6 Characterization of extracellular matrix-derived hydrogel (dECM hydrogel). **a** SEM images of the microarchitecture of dECM hydrogels, prepared from peptic digestion of decellularized trachea for 24, 48, and 72 h (scale bar = 5 μm). **b** Fiber diameters at different peptic digestion times. **c** Interconnectivity of fibers represented by the number of intersection points/μm^2

at shorter digestion times (4 and 12 h), the dECM solution was clear, slightly viscous, and eventually not forming gel. It is possible that monomeric collagen fibrils (molecular weight of 140 kDa) were possibly barely released into the solution (Fig. 6b).

The dECM hydrogel is intended to be used for encapsulating hMSCs and differentiating them to chondrocytes afterward. The dECM solution was a mixture of various tissues (mucosa, submucosa, cartilage, and adventitia) in the trachea that was previously inhabited by different cells in addition to chondrocytes. Therefore, the biological niche of this ECM-rich hydrogel needs further investigation to evaluate the chondrogenic differentiation of hMSCs. In addition, we tested the vascularization of endothelial cells on the dECM hydrogel. The ECM hydrogel served as a biological matrix necessary for HUVEC attachment; however, it did not induce tube-like formation in HUVECs. We demonstrated that the dECM hydrogel supported HUVEC viability longer than Matrigel®. The HUVECs disintegrated and detached from Matrigel® by 24 h, while they could spread nicely on

the ECM hydrogel and a commercially available fibrin gel prepared from bovine plasma. The dECM hydrogel in this study possibly contained biochemical profiles similar to the fibrin gel more than Matrigel®, which is made from mouse sarcoma ECM proteins. Therefore, the dECM hydrogel is able to encapsulate hMSCs and shows promise in potentially forming cartilage rings, but the challenge lies in finding a way to incorporate vessels into the trachea.

The intricate tissue architecture of the dTrachea is hard to replicate by current biofabrication technologies. The present study encountered the challenge of decellularizing cartilage rings, which contain a dense ECM. Within the ECM, lacunae—cavities that trap cell-chondrocytes—proved resistant to the decellularization process (Fig. 2a), potentially triggering an immune response. Further investigations are needed to examine the immune response following implantation. While our study did not investigate ciliated cells differentiation of epithelial cells or chondrogenic differentiation of hMSCs, we focused on the preparation of biomaterials and demonstrated short-term culture for 3, 7 or 14 days (Epithelial cells, Fig. 7; hMSCs and HUVECs, Fig. 8). These
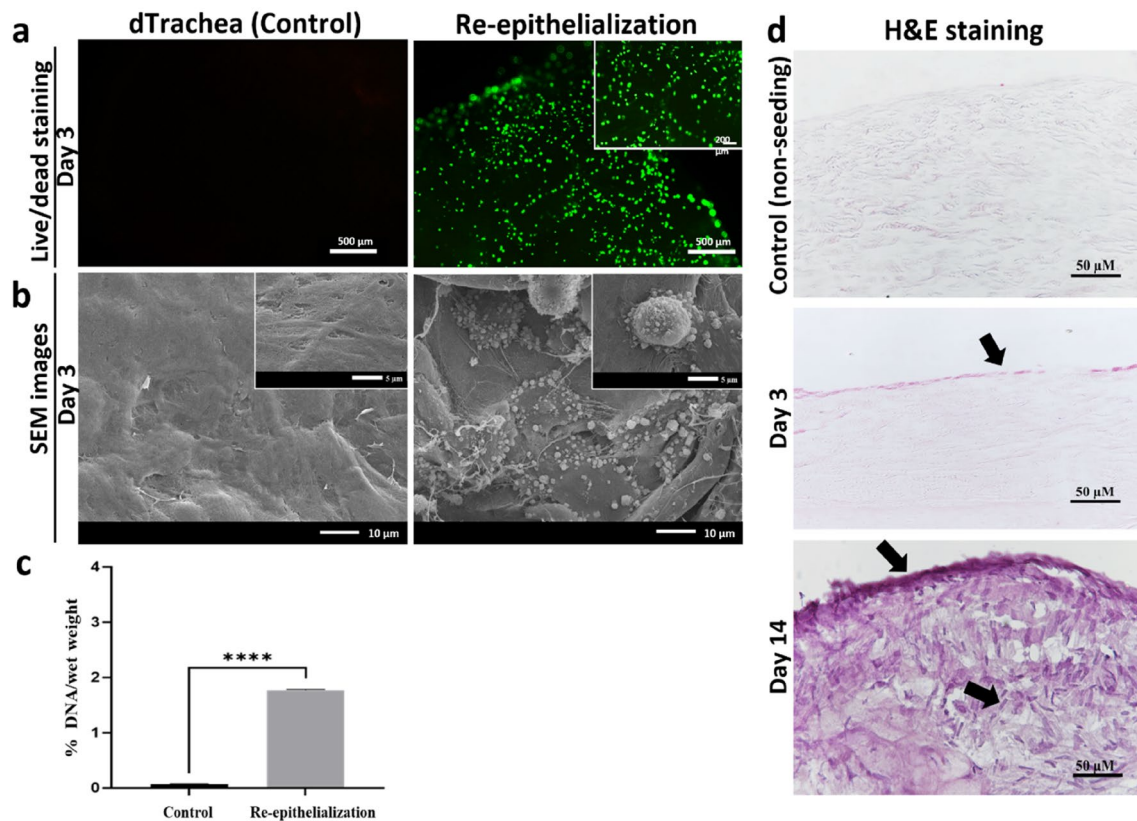
Fig. 7 Re-epithelialization of the decellularized trachea. **a** Primary HBEpCs were seeded on the decellularized trachea for 3 days. Live cells (green) and dead cells (red) (Scale bars = 500 μm). **b** Scanning electron micrographs of the decellularized trachea without and with primary HBEpCs for 3 days (scale bars = 10 and 5 μm). **c** DNA con-tents of the cell-seeded constructs on 3 days. Control, decellularized trachea; re-epithelialization, HBEpCs seeded on the decellularized trachea, ****$P < 0.0001$. **d** The H&E staining of HBEpC on decel-lularized constructs at day 3 and 14. Control, non-seeding trachea. Arrows indicate seeded HBEpCs. Scale bars = 50 μm

findings contribute valuable data for future examining the ciliated cells lining the tracheal interior and exploring the growth and development of cartilage rings, which are crucial for maintaining proper tracheal function. We expect that, in future study of tracheal tissue engineering, the right struc-ture and biochemical niche of decellularized scaffolds will lead to the right tracheal functions, including filtration of particles from the air, open passage for air to travel to and from the lung without collapsing, and mucociliary escalator.

Conclusion

The intricate tissue architecture of the trachea presents a challenge for current biofabrication technologies to replicate accurately. However, decellularized trachea shows promise for restoring tracheal structure without eliciting an immune reaction, as it effectively removes DNA content and major

histocompatibility complex (MHC). The expectation is that the appropriate structure and biochemical niche provided by the dTrachea will support the proper functioning of the trachea. To explore the versatility of decellularized trachea in airway regenerative medicine, this study utilized tracheal ECM to create two types of cell carriers for three distinct cell types: epithelial cells, hMSCs, and HUVECs. In the future, decellularized trachea will serve as a valuable tool for examining ciliated cells lining the tracheal lumen and studying the growth and development of the cartilage rings.

Although HUVECs did not form tube-like structures as an indicator of vascularization, they displayed excellent via-bility and spread out on the dECM hydrogel surface instead. Therefore, the preparation of this dTrachea as dual cell-car-rier systems facilitates re-epithelization and cell encapsula-tion for tracheal reconstruction. This research may pave the way for more effective approaches to develop biomaterial for
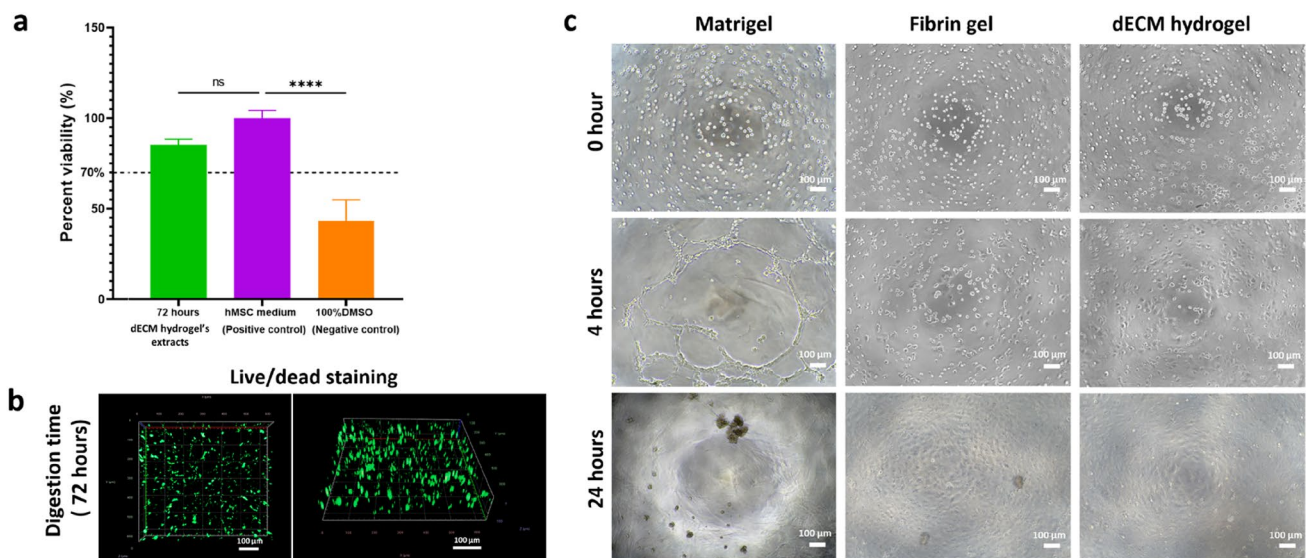
Fig. 8 Cell encapsulation in dECM hydrogels. **a** The metabolic activity of hMSCs cultured in extracts of dECM hydrogel, prepared from peptic digestion of decellularized trachea (dTrachea) for 72 h, was determined by the PrestoBlue™ assay. hMSC medium, positive control; 100% DMSO, negative control. Data are displayed as mean ± standard deviation ($n=3$). **b** hMSCs embedded in dECM hydrogels at day 3. Scale bar = 100 μm. **c** Tubular formation assay of HUVECs on Matrigel®, fibrin gel, and dECM hydrogel. Scale bar = 100 μm

tracheal tissue reconstruction. Our findings contribute valuable insights to the ongoing efforts in tracheal tissue engineering, moving us closer to clinical applications that can benefit patients in need of tracheal repair and regeneration.

Declarations

Conflict of interest The authors declare that they have no known competing financial interests or personal relationships that could have appeared to influence the work reported in this paper.

Ethical Approval Canine tracheae for decellularization were harvested under sterile conditions from canine cadaver, donated for anatomy class of the Faculty of Veterinary science, Chulalongkorn University, Thailand. Animal surgery and husbandry were performed by the Thailand guidelines on the use of experimental animals (ANIMALS FOR SCIENTIFIC PURPOSES ACT, B.E. 2558 (A.D. 2015). This study was approved by the Institutional Animal Care and Use Committee (IACUC) of Chulalongkorn University (No. 2231001).

References

1. Dhasmana, A., A. Singh, and S. Rawal. Biomedical grafts for tracheal tissue repairing and regeneration "Tracheal tissue engineering: an overview." *J. Tissue Eng. Regen. Med.* 14:653–672, 2020.
2. Furlow, P. W. M., and J. Douglas. Surgical anatomy of the trachea. *Ann. Cardiothorac. Surg.* 7:255–260, 2018.
3. Soriano, L., T. Khalid, D. Whelan, et al. Development and clinical translation of tubular constructs for tracheal tissue engineering: a review. *Eur. Respir. Rev.* 30:210154, 2021.
4. Etienne, H., D. Fabre, A. G. Caro, et al. Tracheal replacement. *Eur. Respir. J.* 51:1702211, 2018.
5. Bogan, S. L., G. Z. Teoh, and M. A. Birchall. Tissue engineered airways: a prospects article. *J. Cell. Biochem.* 117:1497–1505, 2016.
6. Crowley, C., M. Birchall, and A. M. Seifalian. Trachea transplantation: from laboratory to patient. *J. Tissue Eng. Regen. Med.* 9:357–367, 2015.
7. Torre, M., P. Varela, D. Romero, and E. Leopold. Complex tracheal resection in children: myths, reality and lessons learned. In Semin Pediatr Surg. Elsevier, 2021, p. 151059.
8. Fishman, J. M., K. Wiles, M. W. Lowdell, et al. Airway tissue engineering: an update. *Expert Opin. Biol. Ther.* 14:1477–1491, 2014.
9. Edward, C., and L. W. Richard. Surgical stapling device–tissue interactions: what surgeons need to know to improve patient outcomes. *Med. Dev. (Auckl).* 7:305–318, 2014.
10. Stefan, W., and E. Weam. Management of tracheobronchial injuries. *J. Thorac. Dis.* 12:6143–6151, 2020.
11. Jin, S., and I. Sugitani. Narrative review of management of thyroid surgery complications. *Gland Surg.* 10:1135–1146, 2021.
12. Kang, Y., C. Wang, Y. Qiao, et al. Tissue-engineered trachea consisting of electrospun patterned sc-PLA/GO-g-IL fibrous

membranes with antibacterial property and 3D-printed skeletons with elasticity. *Biomacromolecules*. 20:1765–1776, 2019.

13. Wu, T., H. Zheng, J. Chen, et al. Application of a bilayer tubular scaffold based on electrospun poly (l-lactide-co-caprolactone)/collagen fibers and yarns for tracheal tissue engineering. *J. Mater. Chem. B*. 5:139–150, 2017.

14. Okamoto, T., Y. Yamamoto, M. Gotoh, et al. Cartilage regeneration using slow release of bone morphogenetic protein-2 from a gelatin sponge to treat experimental canine tracheomalacia: a preliminary report. *ASAIO J*. 49:63–69, 2003.

15. Yamamoto, Y., T. Okamoto, M. Goto, et al. Experimental study of bone morphogenetic proteins-2 slow release from an artificial trachea made of biodegradable materials: evaluation of stenting time. *ASAIO J*. 49:533–536, 2003.

16. Hsieh, C.-T., C.-Y. Liao, N.-T. Dai, et al. 3D printing of tubular scaffolds with elasticity and complex structure from multiple waterborne polyurethanes for tracheal tissue engineering. *Appl. Mater. Today*. 12:330–341, 2018.

17. Liao, J., Q. Guo, B. Xu, and X. Li. Overview of decellularized materials for tissue repair and organ replacement. In: Decellularized Materials, 2021, pp. 1–67.

18. Abdul-Al, M., G. K. Kyeremeh, M. Saeinasab, et al. Stem cell niche microenvironment: review. *Bioengineering (Basel)*. 8:108, 2021.

19. Tong, Z., L. Jin, J. M. Oliveira, et al. Adaptable hydrogel with reversible linkages for regenerative medicine: dynamic mechanical microenvironment for cells. *Bioact Mater*. 6:1375–1387, 2021.

20. Barbulescu, G. I., F. M. Bojin, V. L. Ordodi, et al. Decellularized extracellular matrix scaffolds for cardiovascular tissue engineering: current techniques and challenges. *Int. J. Mol. Sci*. 23:13040, 2022.

21. Zhang, W., A. Du, S. Liu, et al. Research progress in decellularized extracellular matrix-derived hydrogels. *Regen. Ther*. 18:88–96, 2021.

22. Zhu, D., Z. Jiang, N. Li, et al. Insights into the use of genetically modified decellularized biomaterials for tissue engineering and regenerative medicine. *Adv. Drug Deliv. Rev*. 188:114413, 2022.

23. Mendibil, U., R. Ruiz-Hernandez, S. Retegi-Carrion, et al. Tissue-specific decellularization methods: rationale and strategies to achieve regenerative compounds. *Int. J. Mol. Sci*. 21:5447, 2020.

24. Brown, M., J. Li, C. Moraes, et al. Decellularized extracellular matrix: New promising and challenging biomaterials for regenerative medicine. *Biomaterials*. 289:121786, 2022.

25. Ohata, K., and H. C. Ott. Human-scale lung regeneration based on decellularized matrix scaffolds as a biologic platform. *Surg. Today*. 50:633–643, 2020.

26. Badileanu, A., C. Mora-Navarro, A. M. Gracioso Martins, et al. Fast automated approach for the derivation of acellular extracellular matrix scaffolds from porcine soft tissues. *ACS Biomater. Sci. Eng*. 6:4200–4213, 2020.

27. Ye, C., J. Chen, Y. Qu, et al. Naringin in the repair of knee cartilage injury via the TGF-β/ALK5/Smad2/3 signal transduction pathway combined with an acellular dermal matrix. *JOT*. 32:1–11, 2022.

28. Sensi, F., E. D'angelo, A. Biccari, et al. Establishment of a human 3D pancreatic adenocarcinoma model based on a patient-derived extracellular matrix scaffold. *Transl. Res*. 253:57–67, 2022.

29. Biehl, A., A. M. G. Martins, Z. G. Davis, et al. Towards a standardized multi-tissue decellularization protocol for the derivation of extracellular matrix materials. *Biomater Sci*. 11:641–654, 2023.

30. Frey, A., L. P. Lunding, J. C. Ehlers, et al. More than just a barrier: the immune functions of the airway epithelium in asthma pathogenesis. *Front. Immunol*. 11:761, 2020.

31. Hansson, G. C. Mucus and mucins in diseases of the intestinal and respiratory tracts. *J. Intern. Med*. 285:479–490, 2019.

32. Zhang, H., W. Fu, and Z. Xu. Re-epithelialization: a key element in tracheal tissue engineering. *Regen. Med*. 10:1005–1023, 2015.

33. Minnich, D. J., and D. J. Mathisen. Anatomy of the trachea, carina, and bronchi. *Thorac. Surg. Clin*. 17:571–585, 2007.

34. Elliott, M. J., P. De Coppi, S. Speggiorin, et al. Stem-cell-based, tissue engineered tracheal replacement in a child: a 2-year follow-up study. *Lancet*. 380:994–1000, 2012.

35. Elliott, M. J., C. R. Butler, A. Varanou-Jenkins, et al. Tracheal replacement therapy with a stem cell-seeded graft: lessons from compassionate use application of a GMP-compliant tissue-engineered medicine. *Stem Cells Transl. Med*. 6:1458–1464, 2017.

36. Hamilton, N., M. Kanani, D. Roebuck, et al. Tissue-engineered tracheal replacement in a child: a 4-year follow-up study. *Am. J. Transplant*. 15:2750–2757, 2015.

37. Baiguera, S., C. Del Gaudio, E. Kuevda, et al. Dynamic decellularization and cross-linking of rat tracheal matrix. *Biomaterials*. 35:6344–6350, 2014.

38. Shin, Y. S., J. W. Choi, J.-K. Park, et al. Tissue-engineered tracheal reconstruction using mesenchymal stem cells seeded on a porcine cartilage powder scaffold. *Ann. Biomed. Eng*. 43:1003–1013, 2015.

39. Sun, F., Y. Jiang, Y. Xu, et al. Genipin cross-linked decellularized tracheal tubular matrix for tracheal tissue engineering applications. *Sci. Rep*. 6:1–12, 2016.

40. Giraldo-Gomez, D. M., S. J. García-López, L. Tamay-de-Dios, et al. Fast cyclical-decellularized trachea as a natural 3D scaffold for organ engineering. *Mater. Sci. Eng. C*. 105:110142, 2019.

41. Lee, J. S., J. Park, D.-A. Shin, et al. Characterization of the biomechanical properties of canine trachea using a customized 3D-printed apparatus. *Auris Nasus Larynx*. 46:407–416, 2019.

42. Batioglu-Karaaltin, A., M. V. Karaaltin, E. Ovali, et al. In vivo tissue-engineered allogenic trachea transplantation in rabbits: a preliminary report. *Stem Cell Rev. Rep*. 11:347–356, 2015.

43. Butler, C. R., R. E. Hynds, C. Crowley, et al. Vacuum-assisted decellularization: an accelerated protocol to generate tissue-engineered human tracheal scaffolds. *Biomaterials*. 124:95–105, 2017.

44. Lange, P., K. Greco, L. Partington, et al. Pilot study of a novel vacuum-assisted method for decellularization of tracheae for clinical tissue engineering applications. *J. Tissue Eng. Regen. Med*. 11:800–811, 2017.

45. Luo, Y., and L. Ma. Bioprosthetic heart valves with reduced immunogenic residuals using vacuum-assisted decellularization treatment. *Biomed. Mater*. 15:065012, 2020.

46. Pouliot, R. A., B. M. Young, P. A. Link, et al. Porcine lung-derived extracellular matrix hydrogel properties are dependent on pepsin digestion time. *Tissue Eng. C*. 26:332–346, 2020.

47. Visscher, D. O., H. Lee, P. P. van Zuijlen, et al. A photo-crosslinkable cartilage-derived extracellular matrix bioink for auricular cartilage tissue engineering. *Acta Biomater*. 121:193–203, 2021.

48. Yodmuang, S., S. L. McNamara, A. B. Nover, et al. Silk microfiber-reinforced silk hydrogel composites for functional cartilage tissue repair. *Acta Biomater*. 11:27–36, 2015.

49. López-Martínez, S., H. Campo, L. de Miguel-Gómez, et al. A natural xenogeneic endometrial extracellular matrix hydrogel toward improving current human in vitro models and future in vivo applications. *Front. Bioeng. Biotechnol*. 9:156, 2021.

50. Kang, H.-W., S. J. Lee, I. K. Ko, et al. A 3D bioprinting system to produce human-scale tissue constructs with structural integrity. *Nat. Biotechnol*. 34:312–319, 2016.

51. Matias, G. S., A. C. Carreira, V. F. Batista, et al. Ionic detergent under pressure-vacuum as an innovative strategy to generate canine tracheal scaffold for organ engineering. *Cells Tissues Organs*. 212:535–545, 2022.

52. Ravindra, A., W. D'Angelo, L. Zhang, et al. Human bronchial epithelial cell growth on homologous versus heterologous tissue extracellular matrix. *J. Surg. Res*. 263:215–223, 2021.

53. Saldin, L. T., M. C. Cramer, S. S. Velankar, et al. Extracellular matrix hydrogels from decellularized tissues: structure and function. *J Acta Biomater.* 49:1–15, 2017.

54. Tsou, Y.-H., J. Khoneisser, P.-C. Huang, and X. Xu. Hydrogel as a bioactive material to regulate stem cell fate. *Bioactive Mater.* 1:39–55, 2016.

55. Balestrini, J. L., A. L. Gard, K. A. Gerhold, et al. Comparative biology of decellularized lung matrix: implications of species mismatch in regenerative medicine. *Biomaterials.* 102:220–230, 2016.

56. Zhong, Y., W. Yang, Z. Yin Pan, et al. In vivo transplantation of stem cells with a genipin linked scaffold for tracheal construction. *J. Biomater. Appl.* 34:47–60, 2019.

57. Kokubun, K., D. Pankajakshan, M. J. Kim, and D. K. Agrawal. Differentiation of porcine mesenchymal stem cells into epithelial cells as a potential therapeutic application to facilitate epithelial regeneration. *J. Tissue Eng. Regen. Med.* 10:E73–E83, 2016.

58. Kobayashi, K., T. Suzuki, Y. Nomoto, et al. A tissue-engineered trachea derived from a framed collagen scaffold, gingival fibroblasts and adipose-derived stem cells. *Biomaterials.* 31:4855–4863, 2010.

59. Hulmes, D. Collagen diversity, synthesis and assembly. In: Collagen, edited by P. Fratzl. Boston: Springer, 2008, pp. 15–47.